Formation of graphene and hexagonal boron nitride on Rh(111) studied by in-situ scanning tunneling microscopy

Dong, G.

Chapter 10 Rh island formation induced by graphene growth

10.1 Introduction

One of the interesting phenomena already mentioned in the previous chapter was the formation of double-layer Rh island structures by an enclosing graphene monolayer. The origin of these structures will be discussed in more detail in the present chapter.

10.2 Experiment

In Fig. 10.1 and Fig. 10.2, two examples are given of the condensation of Rh adatoms into Rh islands. The sample was prepared by graphene seeding (annealing a pre-deposited sample from room temperature to 975K) and further ethylene deposition, as in previous chapters. The STM images are from the same sequence as the one shown in Fig. 8.3. The images and cross sections in Fig. 10.1 and Fig. 10.2 show that the average height of those Rh areas that were fully enclosed by the growing graphene, increased gradually, as the graphene growth made these areas shrink. This gradual increase in height suggests that the enclosed Rh areas carried a mobile, two-dimensional (lattice) gas of some species other than carbon, of which the density increased as the areas were forced to shrink. Eventually, the density of this mobile overlayer reached a critical value, at which an island was nucleated on each of the enclosed Rh areas. This mobile surface species cannot have originated from the residual gas, because of the low base pressure of the UHV chamber and the high purity of the ethylene gas. The only possibility is that it consisted of Rh adatoms created by the anti-step flow mechanism (Chapter 9), prior to the closure of the perimeter of a hole in the graphene overlayer. The

final height of the islands, at the point where the graphene front came to a standstill, fitted reasonably with the height expected for two layers of Rh (Fig. 10.1(C & D) and Fig. 10.2(C & D)), supporting our conclusion that they consisted completely of Rh and that the mobile overlayer, present before this nucleation, also consisted of Rh adatoms, confined by the surrounding graphene edges. Since graphene prefers Rh steps as nucleation sites, geometries in which Rh adatoms are confined by graphene should occur frequently. The confinement can easily lead to situations in which the local density of Rh adatoms is significantly above the equilibrium Rh adatom density on Rh(111) at the graphene growth temperature.

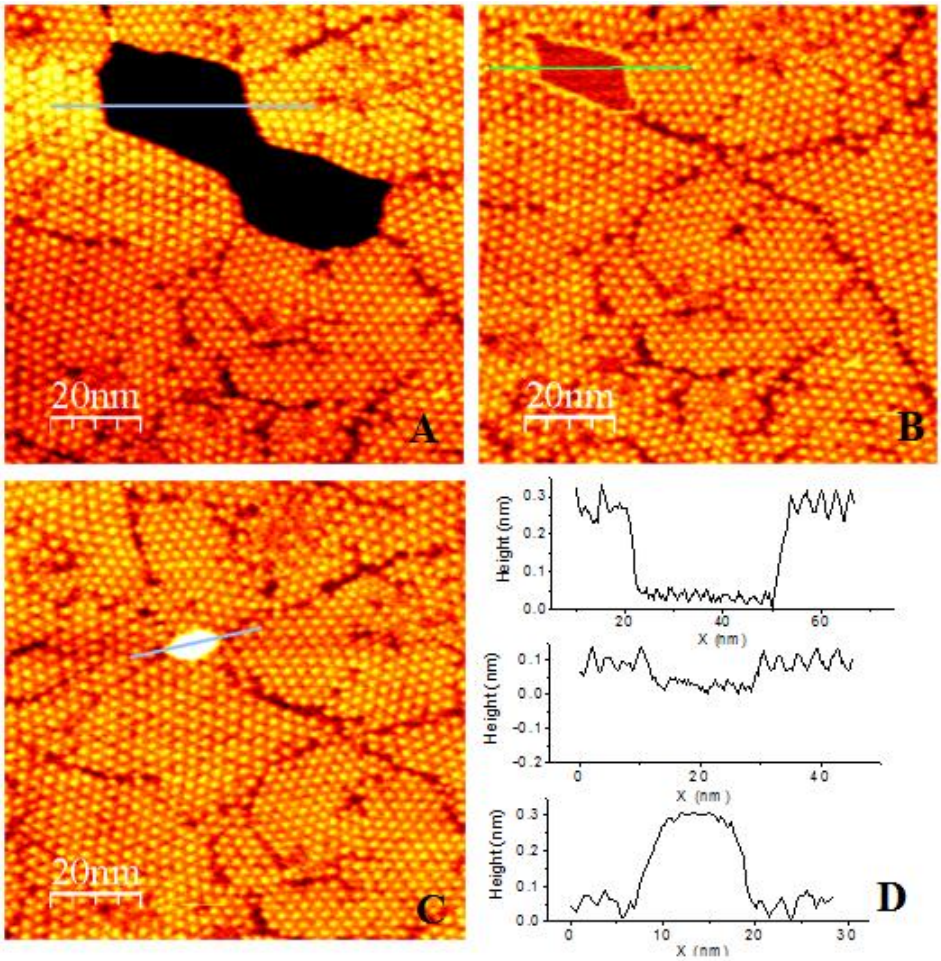

Fig. 10.1 STM images of confinement and nucleation of Rh adatoms due to graphene growth. (A) The starting situation of the graphene overlayer that encloses a bare region of Rh substrate. The concentration of Rh adatoms is still low. (B) The same area after 367 seconds of ethylene deposition at two pressures, of 0.56 x 10^{-8} and 1.4 x 10^{-8}. The apparent height of the enclosed Rh area increased, which we attribute to the increase in the concentration of Rh adatoms. (C) The final state of the vacancy island: a two-layer high Rh island has been formed by the adatoms. (D) Height profiles along the lines in images A, B, and C (top to bottom). With respect to the original level of the enclosed Rh area, the heights have increased by almost zero in A, approximately 0.2 nm in B, and 0.5 nm, corresponding to 2 layers of Rh in C. The STM images all had a size of 100 nm × 100 nm, and have been taken at a sample voltage of V_b = -1.84 V and a tunneling current of I_t = 0.05 nA.

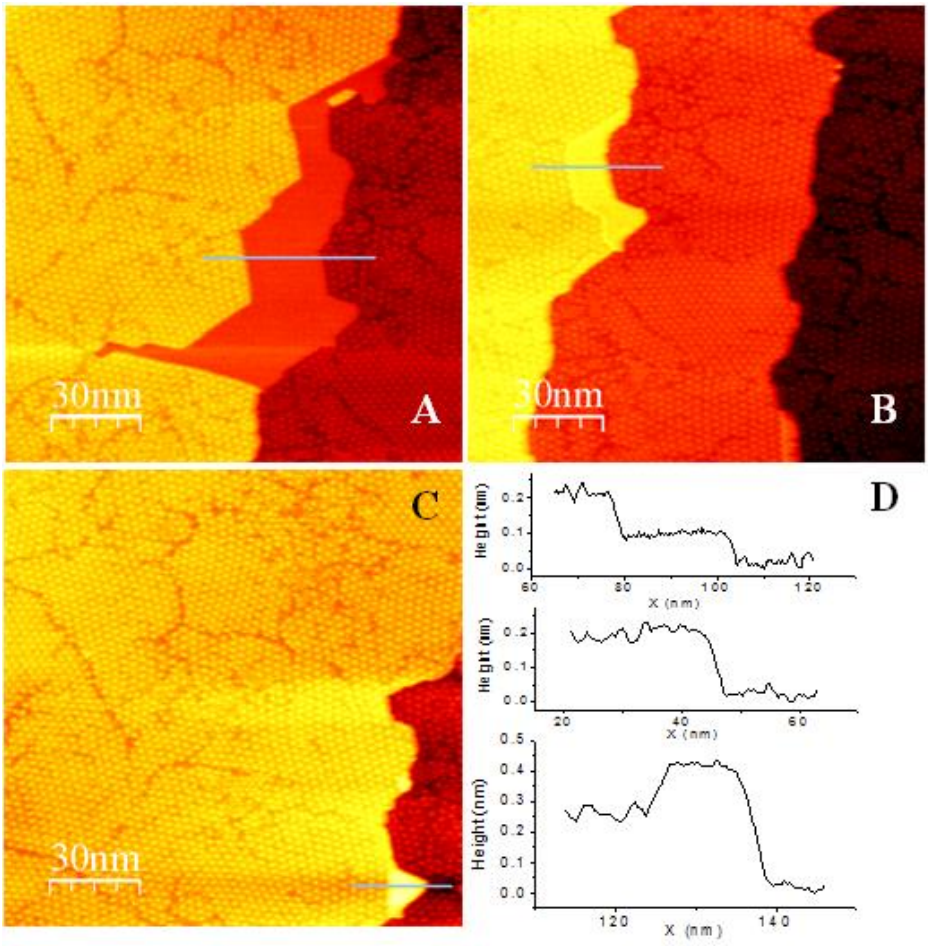

Fig. 10.2 STM images of confinement and nucleation of Rh adatoms due to graphene growth. (A) The starting situation of the graphene overlayer. The concentration of Rh adatoms is still low. (B) The same area after 761 seconds of ethylene deposition at pressures varying from 1.4 x 10^{-8} to 7.8 x 10^{-8} mbar. The apparent height of the enclosed Rh area increased, which we attribute to the increase in the concentration of Rh adatoms. (C) The final state of the vacancy island: a two-layer high Rh island has been formed by the adatoms. (D) Height profiles along the lines in images A, B, and C (top to bottom). With respect to the original level of the Rh substrate, the height of the enclosed Rh area had increased from almost 0.06 nm in A, approximately 0.2 nm in B, and 0.5 nm, corresponding to 2 layers of Rh in C.
The STM images all have a size of 150 nm × 150 nm, and have been taken at a sample voltage of V_b = -1.84V and a tunneling current of I_t = 0.05 nA.

10.3 Tunneling current vs. adatom density

In an attempt to analyze the observations more quantitatively, we first calculate the relation between the density of Rh adatoms and the apparent height in the STM images. We start from the following, simple expression for the tunneling current I over a flat piece of Rh surface.

$$I = Ae^{-\sqrt{\phi}S} \qquad \text{Eq.10.1}$$

A is a constant, Φ is the mean work function, S is the distance between tip and sample and the units have been chosen such Φ (eV), S (Å) as to avoid additional factors in the exponent. In order to incorporate the effect of a sub-monolayer quantity of mobile Rh adatoms, we make several simplifying assumptions. Firstly, we assume that the work function above an adatom is identical to that above a flat part of the Rh surface. Secondly, we assume that each individual adatom locally changes the tunneling current as if it were a portion of a flat Rh surface, one atomic layer above the original surface. Our third assumption is that the tip exhibits a negligible force on the Rh adatoms, so that the average adatom density directly below the tip is equal to that elsewhere on the investigated Rh surface. Our final assumption is that the diffusion rate of the Rh adatoms is too high for the STM feedback loop to react to individual hopping events of Rh adatoms into and out of the tunneling gap. The consequence of the latter assumption is that the height to which the feedback loop regulates the tip is the one that corresponds with the time-averaged value of the tunneling current. This average tunneling current on a surface with a coverage θ of Rh adatoms can be written as:

$$I = (1-\theta)Ae^{-\sqrt{\phi}S} + \theta Ae^{-\sqrt{\phi}(S-H)} \qquad \text{. Eq. 10.2}$$

H is the effective height of an adatom, which we associate with the interlayer spacing of the Rh crystal. When the STM is running in the constant current mode, the tip will withdraw over an additional distance h with respect to the initial tip-surface separation S_0 over a piece of Rh terrace without Rh adatoms, in order to compensate for the current increase caused by diffusing adatoms. This gives the following condition on h.

$$Ae^{-\sqrt{\phi}S_0} = (1-\theta)Ae^{-\sqrt{\phi}(S_0+h)} + \theta Ae^{-\sqrt{\phi}(S_0+h-H)} \quad \text{Eq. 10.3}$$

Solving it provides us with the following relation between the apparent height h and the Rh adatom coverage θ:

$$h = \frac{\ln[(1-\theta)+\theta e^{\sqrt{\phi}H}]}{\sqrt{\phi}} \quad \text{Eq. 10.4}$$

Substituting the values Φ = 5.4 eV [95, 96] for the work function and H = 2.2 Å for interlayer spacing of Rh(111), we obtain the solid line in Fig. 10.3.

In the above calculation, it was assumed that the work function (apparent barrier) is constant. In reality the work function is known to depend on the distance between tip and sample, and on the roughness of the sample [97]. Both of these factors actually lower the apparent barrier. We therefore should anticipate an increase the tunneling current in the presence of adatoms. In an attempt to incorporate this effect, we assume that the apparent barrier is lowered from the original value of Φ_0 to Φ_1, when the tip is above an adatom. This leads to a modest modification of Eq. 10.4

$$Ae^{-\sqrt{\phi_0}S_0} = (1-\theta)Ae^{-\sqrt{\phi}_0(S_0+h)} + \theta Ae^{-\sqrt{\phi_1}(S_0+h-H)}$$

$$\theta = \frac{1-e^{\sqrt{\phi}_0 h}}{1-e^{(\sqrt{\phi}_0-\sqrt{\phi_1})(S_0+h)+H\sqrt{\phi_1}}} \quad \text{Eq. 10.5}$$

Strictly speaking, in the first term on the right side the barrier should be increased with respect to Φ_0, but this increase is more modest than the decrease of Φ_1 with respect to Φ_0 [97]. So we here took the work function in the first term as Φ_0. The precise value of Φ_1 and S_0 does not influence the discussion below. So we took estimated values for them .The result for a Φ_1-value of 4.5 eV and S_0 of 0.5 nm is shown in Fig. 10.3 as the dashed curve. Of course, Eq. 10.5 properly accounts for variations in the barrier only for low coverages, where h is still small. At coverages approaching unity, Eq. 10.4 should be more appropriate. In other words, we should expect behavior that follows the dashed curve for low θ-values and crosses over to the solid curve at higher θ.

10.4 Models

We confront the two model calculations in Fig. 10.3 with the measured heights of the enclosed Rh region shown in the images of Fig. 10.1 and Fig. 10.2. From the final state (Fig. 10.1C), with a double-layer Rh island, tightly surrounded by graphene, we precisely know the excess amount of Rh. We assume that in the earlier stages precisely the same amount of Rh was distributed evenly over the bare Rh region in the form of mobile adatoms. This enables us to directly calculate the surface coverage θ in each of the earlier stages from the observed area of the enclosed Rh region. The results of this analysis, combined with the measured apparent heights of the Rh are plotted in Fig. 10.3 as the red and black squares. It is quite obvious that the experimental data do not fit either of the two model calculations very well. Most notably, the two sets of data from different areas do not coincide. Both of the experimental data exhibit a significant offset along the horizontal axis with respect to both calculations that cannot be improved by modifying the functional form of the relation between the apparent barrier and the tip-sample distance. What the experimentally determined heights strongly suggest is that the density of Rh adatoms was close to zero in the initial stages, e.g. in Fig. 10.1A. This is surprising, since this would imply that the density varied more strongly than inversely proportionally to the available area. Closer inspection of the images revealed that the graphene edge, i.e. the inner contour of the enclosed Rh area, was decorated by a protrusion. If this decorating line were to consist of Rh atoms, we could easily explain the θ-offset in the experimental data in Fig. 10.3. Assuming that at each stage, the inner contour of the graphene was decorated by a single row of Rh atoms with an interatomic distance of 0.269 nm, typical for Rh, we recalculated the coverages of the enclosed Rh areas with the remaining, mobile Rh adatoms. This procedure resulted in the red squares in Fig. 10.4. Also data for the Rh region in Fig. 10.2; in that case only part of the Rh region is enclosed by a (decorated) graphene edge, the remainder of the contour being a step in the Rh itself. The same procedure brings these data (black squares) nicely in line with those from the enclosed Rh area in Fig. 10.1. Both data sets are in nearly quantitative agreement with the two model calculations.

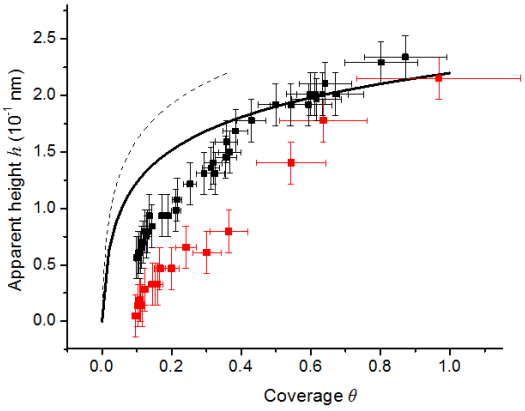

Fig. 10.3 Comparison between the experiment of Fig. 10.1 and two simple model calculations for the relation between the apparent height in the STM images and the density of adatoms. The solid line is from Eq. 10.4 and the dashed line is from Eq.10.5, in which the work function reduction due to the reduced tip-sample distance is considered. A more complete description should lie between these lines. The experimental heights, obtained from the region considered in Fig. 10.1 and in Fig. 10.2, are plotted as the red and black squares with error bars**.**

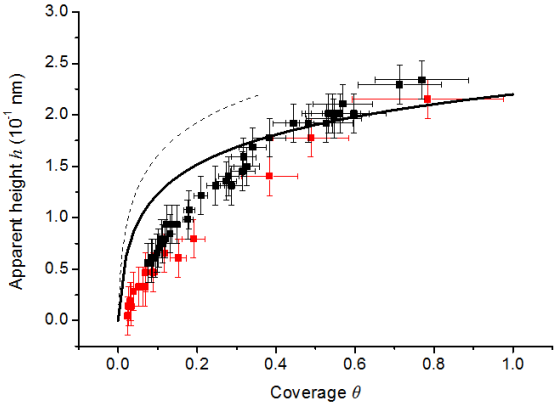

Fig. 10.4 Relation between the apparent height in STM and the density of adatoms. The solid line is from Eq. 10.4. The dashed line is from Eq. 10.5. The red squares are experimental data from the enclosed Rh area in Fig. 10.1, and the black ones are from the enclosed Rh area in Fig. 8.2. The Rh adatom density was calculated assuming that the graphene edges were all decorated by a single row of Rh atoms with an inter-atomic distance of 0.269 nm. Of the enclosed Rh area in Fig. 10.2, only the graphene edge is considered to be covered by a Rh line, rather than the entire contour around the Rh area.

10.5 Conclusion

The analysis presented in this chapter demonstrates that the edges of the growing graphene are saturated by one atomic line of Rh. Apparently, the bonding to the graphene edge makes the free energy for a Rh atom at the edge lower than that of a Rh adatom. Interestingly, this line of Rh does not have the properties of bulk Rh. We do not observe nucleation of Rh islands at the Rh-decorated graphene edges, even though the edges might seem to present an excellent nucleus. We ascribe this behavior to the strong bonding that the edge Rh atoms have to the carbon atoms at the graphene edge. We also suggest that this line of Rh may play a role in the energy barriers for graphene attachment and detachment [51, 53, 98].